ISSN 1028-334X, Doklady Earth Sciences, 2009, Vol. 429A, No. 9, pp. 1496–1500. © Pleiades Publishing, Ltd., 2009.
Original Russian Text © N.A. Krivolutskaya, A.V. Sobolev, D.V. Kuzmin, N.M. Svirskaya, 2009, published in Doklady Akademii Nauk, 2009, Vol. 429, No. 4, pp. 518–522.

GEOCHEMISTRY

Unique Zoned Olivines from an Ultrabasic—Basic Massif in the Noril'sk Disitrict

N. A. Krivolutskaya[a], Corresponding Member of the RAS A. V. Sobolev[a, b], D. V. Kuzmin[a, b], and N. M. Svirskaya[c]

Received June 24, 2009

DOI: 10.1134/S1028334X09090189

The specifics of the morphology, internal structure, and composition of olivine, one of the major rock-forming minerals of ultrabasic and basic rocks, contains valuable information on the conditions of its formation and are widely used in petrology [11, 8, 3, 7, 12]. One of its important characteristics is zoning, which is most pronounced in lunar [8] and Martian [2] meteorites. Olivine exhibits both normal and reverse zoning, with the core–rim difference reaching 25 mol % forsterite. However, this phenomenon is uncommon in the terrestrial intrusive rocks, because subsolidus diffusion usually "smoothes out" the initial compositional heterogeneities of the mineral. At present, the available data are reduced to scarce olivine grains with zoned distribution of major (Fe and Mg with Fo gradient of 8–10 mol % [1, 4, 5]) and trace elements Ca, Ni, as well as Al, Cr, and P [4, 9]. Therefore, the find of zoned olivines with the core–rim difference more than 20 mol % Fo in the magmatic rocks of the Noril'sk district is a unique phenomenon not only for this region but also for ultrabasite–basite complexes around the world.

The Noril'sk district is located in the NW Siberian trap province. It consists of the rocks of the crystalline basement and platform cover represented by the Early Cambrian–Late Permian terrigenous–carbonate rocks and Early Triassic basalts. Numerous ultrabasite–basite hypabyssal massifs in the forms of chonoliths and bodies of irregular shape are localized among the sedimentary and volcanic rocks of the area. Distinctly differentiated intrusions are combined into the productive Noril'sk complex, which is characterized by an elevated average weighted MgO content (10–12 wt %) relative to tholeiitic basalts predominant in the section (6–7 wt %). Some of them contain superlarge Pt–Cu–Ni deposits (Talnakh, Oktyabr'skoe, Noril'sk-1), whereas others are either weakly mineralized or barren. Their age relations with volcanic rocks were not established exactly, because in most cases the intrusions are localized in the underlying sedimentary rocks.

One of the representatives of this type of magmatic complexes is the massif studied by us in the eastern part of the area, in the Mikchangda River basin. It is located in the Devonian carbonate–terrigenous rocks and was recovered by borehole MD-48 at a depth of 1157–1257 m during prospecting works of OOO Noril'skgeologiya. From bottom upward, the massif consists of diverse gabbrodolerite varieties: lower contact, lower taxitic, picritic, olivine, olivine-bearing, and upper picritic and contact rocks. The predominant medium-grained doleritic texture of the rocks suggests the hypabyssal conditions of their formation. Olivine occurs practically throughout the entire section of the intrusion, and the morphology and size of its grains change depending on the rock type: high-Mg varieties (picritic gabbrodolerites) are dominated by subeuhedral large crystals (up to 1–2 mm, on average, 0.5 mm) or rounded grains 0.4–0.1 mm, while in the low-Mg rocks it occurs mainly as interstitial between plagioclase crystals (0.2–0.5 mm). Cr-magnetite and ilmenite are subordinate minerals.

The remarkably unusual feature of the massifs of the Noril'sk district is the discovery of olivine with contrast zoning in the rocks of most of the section of the studied intrusion. The zoning was identified by using optical microscopic study and was confirmed by microprobe analyses (Fig. 1). Olivines were analyzed using a JEOL JXA-8200 Superprobe electron microprobe at the Max Planck Institute for Chemistry (Mainz, Germany) using a specially developed technique [13], which allowed a significant increase in the detection limit of trace elements (Ti, Cr, Mn, Co, and Ni) up to 10 ppm. The forsterite mole fraction in olivine was determined accurate to 0.2. The compositions

[a] *Vernadsky Institute of Geochemistry and Analytical Chemistry, Russian Academy of Sciences, ul. Kosygina 19, Moscow, 119091 Russia*
e-mail: nakriv@mail.ru
[b] *Max-Planck-Institute für Chemie, PO Box 3060, 550 Mainz, Germany*
[c] *Sobolev Institute of Geology and Mineralogy, Siberian Branch, Russian Academy of Sciences, pr. Akademika Koptyuga 3, Novosibirsk, 630090 Russia*

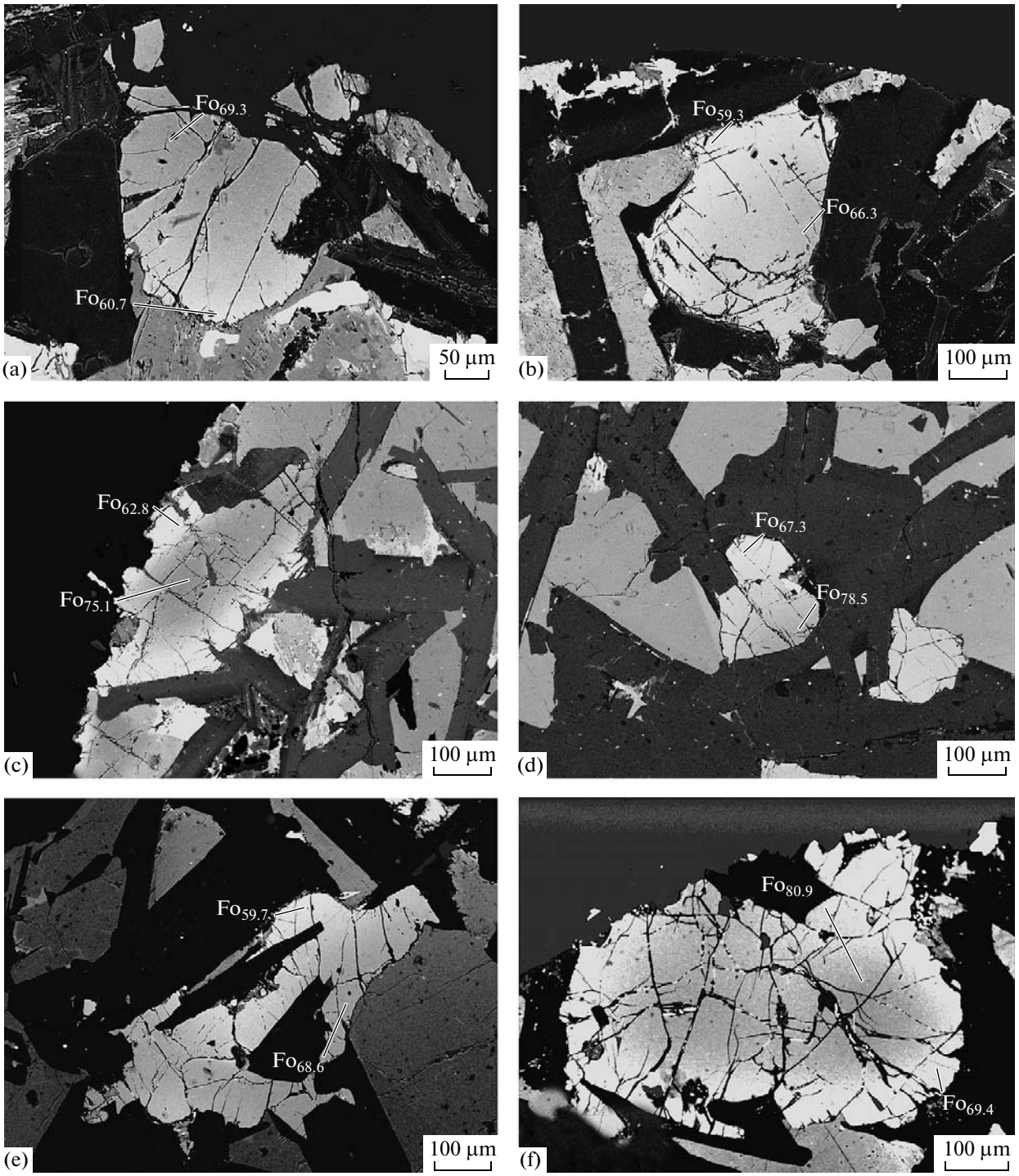

Fig. 1. BSE image of zoned structure of olivine. Samples (numbers correspond to depth along the borehole MD-48): (a) 1212, (b) 1179, (c) 1208, (d) 1217, (e) 1210, (f) 1215.

of the most contrasting zoned olivines from the rocks of different horizons of the intrusion are listed in Table 1.

Most compositionally variable grains were found in the medium-grained and olivine-bearing massive gabbrodolerites with doleritic and poikilophitic texture within a depth range of 1170–1230 m (average MgO content of 7.5 wt %). The Mg# of olivines from one sample for olivine and olivine-bearing rocks varies within 12–20 mol %. The difference between central and marginal zones of the grains can strongly vary within one sample. The maximal core–rim difference was found to be 20.1 mol %. The upper and lower endocontacts of the

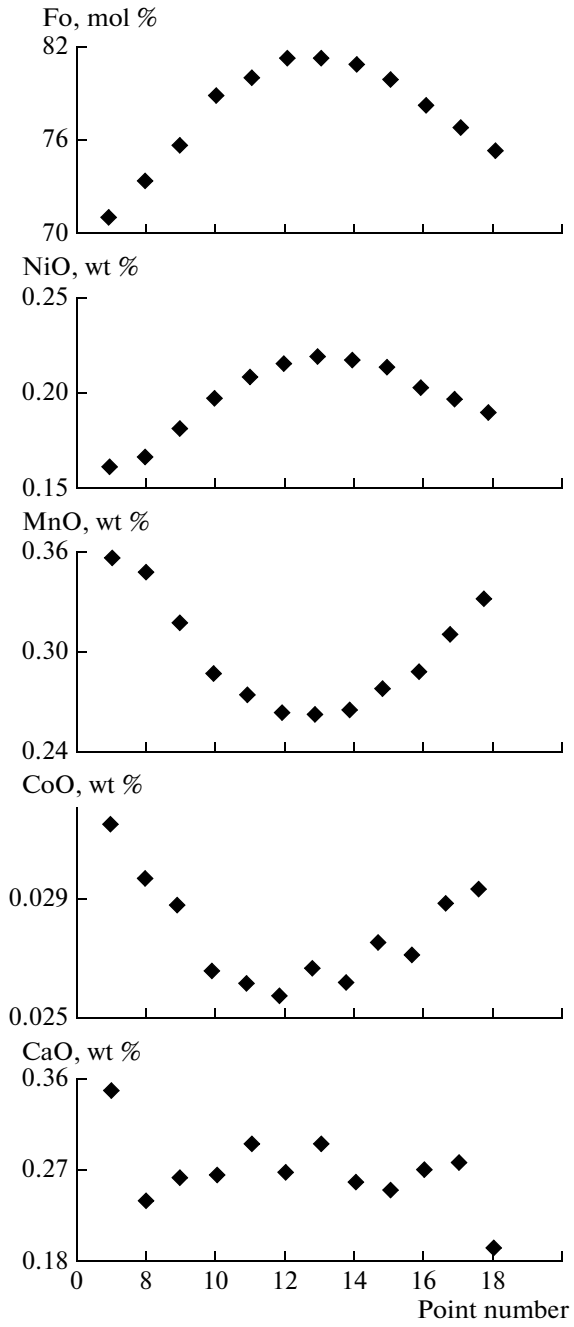

Fig. 2. Variations in trace element contents (wt %) depending on contents of major elements along the profile across zoned olivine based on microprobe data. Distance between points is 100 μm, sample MD-48/1193.

picritic gabbrodolerites (19–22 wt % MgO) contain practically unzoned olivines (Table 1).

The detailed study of rim–core–rim profile of the large olivine grain with a step of 100 μm is shown in Fig. 2. The NiO content has a positive correlation with the forsterite component in the mineral ($R^2 = 0.96$), while the MnO and CoO contents are correlated with the fayalite member ($R^2 = 0.98$ and 0.92, respectively). The CaO content does not depend on the contents of major elements and shows no correlation with Fo ($R^2 = 0.01$). However, olivine grains can show not only symmetrical zoning, as is shown in Fig. 2, but also demonstrate a more complex structure (Fig. 1f). In tight association with plagioclase, olivine has unidirected zoning (Fig. 1).

In order to determine the formation conditions of zoned olivines, equilibrium crystallization was modeled using the COMAGMAT-3.65 program (http://geo.web.ru/~ariskin/soft.html-id=comagmat.htm) for series of samples taken throughout the section. The composition one of them (sample MD-48/1208) is as follows: SiO_2 47.79, TiO_2 1.03, Al_2O_3 15.85, FeO 11.4, MnO 0.16, MgO 7.27, CaO 10.82, Na_2O 2.22, K_2O 0.38, P_2O_5 0.11, L.O.I. 1.44 (analyses were performed by XRF method at the Vernadsky Institute of Geochemistry and Analytical Chemistry, Russian Academy of Sciences, analysts I.A. Roshchina and T.V. Romashova). The rock consists of olivine (up to 10 wt %), plagioclase (35–40 wt %), clinopyroxene (25–30 wt %), subordinate orthopyroxene (2–3%), and Ti-magnetite. Calculations were made for pressure of 1 kbar (since rocks were formed at a depth of no more than 1200 m), and the water content estimated from an element of close compatibility (K_2O content) was taken to be 0.4 wt %. Oxygen fugacity corresponded to NNO–0.5 and was controlled by comparison of calculated data with observed crystallization order in the rock, in particular, by the appearance of ilmenite and magnetite in them.

According to modeling results, plagioclase $An_{80.4}$ was the first liquidus phase to appear during crystallization at $T = 1197$°C; it was almost immediately followed by olivine $Fo_{80.2}$ ($T = 1184$°C). Further temperature decrease led to the crystallization of augite ($En_{43.4}Fs_{14.6}Wo_{41.0}$) at 1135°C, magnetite ($T = 1083$°C), and orthopyroxene ($T = 1066$°C). Of 12 grains measured in this sample, the highest Mg olivine is $Fo_{78.2}$, however, there is a high probability of discovery of a mineral with higher Fo content during more detailed study. In addition, it can be partially re-equilibrated with the melt during temperature decrease. The observed zoning in one of the olivine grains from this sample (Fig. 1d) was formed at temperature gradient as low as 64°C (1152–1088°C, $Fo_{75.4–63.2}$). This olivine is surrounded by plagioclases ($An_{70–72}$), whose composition is very close to that ($An_{70.5}$) calculated at the temperature of the core formation (1152°C).

What are the differences in formation conditions between the considered intrusive rocks and other hyperbasite–basite massifs of the Noril'sk district? The formation of zoned grains was caused by rapid cooling of the rocks, which prevented equilibration of the rim and core compositions. This can be caused by several factors. First, the high rate of crystallization of the massif was provided by the structural position of the studied gabbrodolerites, in particular, their localization in the northern periclinal framing of the rigid

Composition of zoned olivines from the intrusion of the Noril'sk district

Ordinal no.	Depth, m	$Fo_c–Fo_r$	Fo, mol %	SiO_2	TiO_2	FeO	CaO	MnO	MgO	NiO	Cr_2O_3	CoO	Total
1	1161	0.3	79.76	39.22	0.012	19.02	0.15	0.31	42.02	0.15	0.020	0.027	100.96
2			79.48	39.20	0.027	19.36	0.17	0.31	42.07	0.14	0.011	0.025	101.34
3	1171	1.2	66.71	37.18	0.019	29.98	0.22	0.43	33.69	0.12	0.011	0.032	101.69
4			65.48	36.86	0.018	30.80	0.14	0.44	32.77	0.11	0.012	0.033	101.20
5		6.9	66.50	37.41	0.010	29.92	0.41	0.43	33.31	0.09	0.008	0.031	101.66
6			59.56	36.57	0.021	35.42	0.23	0.54	29.26	0.07	0.002	0.035	102.14
7	1193	10.4	70.96	37.69	0.009	26.13	0.35	0.36	35.80	0.16	0.028	0.031	100.48
8			73.23	38.07	0.007	24.43	0.24	0.35	37.48	0.17	0.015	0.030	100.74
9			75.61	38.22	0.006	22.47	0.26	0.32	39.07	0.18	0.016	0.029	100.53
10			78.80	39.00	0.008	19.68	0.26	0.29	41.01	0.20	0.025	0.027	100.45
11			80.01	39.39	0.007	18.71	0.29	0.27	42.01	0.21	0.022	0.026	100.90
12			81.26	39.60	0.006	17.63	0.27	0.26	42.89	0.22	0.029	0.026	100.88
13			81.31	39.34	0.009	17.58	0.29	0.26	42.89	0.22	0.031	0.027	100.59
14			80.92	39.49	0.008	17.92	0.26	0.27	42.63	0.22	0.033	0.026	100.80
15			79.92	39.16	0.008	18.74	0.25	0.28	41.84	0.21	0.027	0.027	100.49
16			78.27	38.92	0.008	19.96	0.27	0.29	40.32	0.20	0.026	0.027	99.97
17			76.85	38.74	0.008	21.35	0.28	0.31	39.76	0.20	0.022	0.029	100.63
18			75.35	38.51	0.011	22.66	0.19	0.33	38.85	0.19	0.025	0.029	100.75
19		10.4	70.96	37.69	0.009	26.13	0.35	0.36	35.80	0.16	0.038	0.031	100.60
20			81.31	39.34	0.009	17.58	0.29	0.26	42.89	0.22	0.031	0.027	100.70
21		20.4	81.30	39.33	0.007	17.59	0.27	0.29	42.90	0.29	0.032	0.026	100.71
22			60.92	35.89	0.022	33.44	0.19	0.48	29.24	0.25	0.005	0.036	99.49
23		17.4	80.48	38.82	0.012	18.10	0.25	0.25	41.86	0.14	0.027	0.025	99.47
24			63.08	36.45	0.027	31.73	0.26	0.46	30.41	0.19	0.008	0.033	99.65
25			68.33	37.98	0.021	27.71	0.30	0.40	33.53	0.16	0.022	0.033	99.13
26	1208	7.2	71.03	37.84	0.027	26.62	0.21	0.38	36.62	0.15	0.029	0.031	101.96
27			63.80	37.16	0.025	32.50	0.22	0.47	32.13	0.09	0.003	0.033	102.66
28		12.1	75.40	38.70	0.012	23.10	0.50	0.31	39.73	0.17	0.052	0.027	102.66
29			63.33	36.95	0.017	32.88	0.13	0.47	31.85	0.12	0.005	0.037	102.46
30	1212	8.5	69.58	37.45	0.013	27.63	0.21	0.40	35.44	0.15	0.010	0.031	101.37
31			61.10	36.46	0.066	34.24	0.22	0.53	30.16	0.13	0.002	0.036	101.85
32		3.5	78.57	38.83	0.009	20.19	0.46	0.28	41.51	0.20	0.106	0.026	101.69
33			75.05	38.34	0.025	23.13	0.24	0.34	39.01	0.16	0.014	0.029	101.31
34	1215	13.4	80.77	38.69	0.011	18.00	0.20	0.26	42.40	0.23	0.030	0.025	99.88
35			67.40	37.51	0.009	29.34	0.88	0.41	34.03	0.14	0.044	0.027	102.45
36	1217	12.9	78.08	38.64	0.015	20.37	0.08	0.31	40.70	0.22	0.008	0.027	100.41
37			65.21	37.11	0.030	30.78	0.18	0.45	32.36	0.19	0.002	0.031	101.15
38	1232	0.6	78.64	38.89	0.013	20.17	0.23	0.30	41.64	0.23	0.027	0.028	101.55
39			78.05	38.94	0.034	20.76	0.18	0.31	41.40	0.24	0.004	0.029	101.92
40	1246	3.1	76.98	38.39	0.027	21.50	0.28	0.34	40.33	0.12	0.003	0.023	101.03
41			73.84	37.97	0.037	24.09	0.28	0.42	38.13	0.11	0.003	0.023	101.08
42		7.6	79.79	39.07	0.021	18.96	0.23	0.31	41.99	0.13	0.007	0.022	100.76
43			72.19	37.47	0.017	25.26	0.10	0.38	36.78	0.11	0.010	0.027	100.18

Note: Depth is the depth, m, along borehole MD-48; Fo is the mole fraction of forsterite in olivine; $Fo_c–Fo_r$ is the difference in the forsterite component between core and rim in olivines.

Khantai–Rybninsk swell, where magma rapidly ascended along systems of vertical fractures and cooled under subsurface conditions. We have no accurate data on the morphology of the massif; however, its thickness could not be higher than 100 m, and, presumably is even thinner due to the inclined attitude of the intrusion. This follows from its internal structure: absence of significant differentiation (typical of subhorizontal bodies) with rapid transition from picritic gabbrodolerites to olivine-free varieties. In contrast, olivine is fairly evenly distributed over its section. Second, an additional factor of rapid cooling of the rocks was the injection of the melt in the unheated host rocks, because this block was not saturated with intrusion bodies, as the Kharaelakh and Noril'sk troughs containing large deposits.

The age of the massif is presently unknown, but it was formed either prior to the main stage of volcanism, or the rocks of the tufflava sequence were thin within the given anticline structure or completely absent. Thus, the formation of the intrusion recovered by borehole MD-48 occurred closely to the paleodenudation surface. At the same time, the intrusion of the massifs in the Noril'sk trough occurred simultaneously during (or immediately after) the formation of basalts.

The indicated combination of geological factors led to the appearance of unique zoned olivines in the ultrabasite–basite intrusion of the area.

ACKNOWLEDGMENTS

This work was supported by the Russian Foundation for Basic Research (project nos. 07-05-01007 and 09-05-01193).

REFERENCES

1. J. Ando, Y. Shibata, Y. Okajima, et al., Nature **414**, 893–895 (2001).
2. A. J. Irving, T. E. Bunch, S. M. Kuehner, et al., Lunar Planet. Sci. **35**, 1444 (2004).
3. C. E. Ford, D. G. Russell, and J. A. Craven, J. Petrol. **24**, 256–265 (1983).
4. V. S. Kamenetsky, M. B. Kamenetskaya, A. V. Sobolev, et al., J. Petrol. **49**, 823–839 (2008).
5. L. M. Larsen and A. K. Pedersen, J. Petrol. **41**, 1071–1098 (2000).
6. M. S. Milman-Barris, J. R. Beckett, M. B. Baker, et al., Contrib. Mineral. Petrol. **155**, 739–765 (2008).
7. H. D. Nathan and C. K. Van Kirk, J. Petrol. **19**, 66–94 (1978).
8. H. Connoly, J. Zipfel, and J. Grossman, Meteorit. Planet. Sci. **41**, 1383–1418 (2006).
9. J. J. Papike, J. M. Karner, and C. K. Shearer, Am. Mineral. **90**, 277–290 (2005).
10. T. H. Pearce, Nature **276**, 771–774 (1978).
11. P. L. Roeder and R. F. Emslie, Contrib. Mineral. Petrol. **29**, 275–289 (1970).
12. A. V. Sobolev, A. W. Hofmann, S. V. Sobolev, et al., Nature **434**, 590–597 (2005).
13. A. V. Sobolev, A. W. Hofmann, and D. V. Kuzmin, Science **316**, 412–417 (2007).